Filopodia are dispensable for endothelial tip cell guidance

Li-Kun Phng[1,2,*], Fabio Stanchi[1,2] and Holger Gerhardt[1,2,3,*]

SUMMARY

Actin filaments are instrumental in driving processes such as migration, cytokinesis and endocytosis and provide cells with mechanical support. During angiogenesis, actin-rich filopodia protrusions have been proposed to drive endothelial tip cell functions by translating guidance cues into directional migration and mediating new contacts during anastomosis. To investigate the structural organisation, dynamics and functional importance of F-actin in endothelial cells (ECs) during angiogenesis *in vivo*, we generated a transgenic zebrafish line expressing Lifeact-EGFP in ECs. Live imaging identifies dynamic and transient F-actin-based structures, such as filopodia, contractile ring and cell cortex, and more persistent F-actin-based structures, such as cell junctions. For functional analysis, we used low concentrations of Latrunculin B that preferentially inhibited F-actin polymerisation in filopodia. In the absence of filopodia, ECs continued to migrate, albeit at reduced velocity. Detailed morphological analysis reveals that ECs generate lamellipodia that are sufficient to drive EC migration when filopodia formation is inhibited. Vessel guidance continues unperturbed during intersegmental vessel development in the absence of filopodia. Additionally, hypersprouting induced by loss of Dll4 and attraction of aberrant vessels towards ectopic sources of Vegfa165 can occur in the absence of endothelial filopodia protrusion. These results reveal that the induction of tip cells and the integration of endothelial guidance cues do not require filopodia. Anastomosis, however, shows regional variations in filopodia requirement, suggesting that ECs might rely on different protrusive structures depending on the nature of the environment or of angiogenic cues.

KEY WORDS: Actin, Filopodia, Endothelial cell, Angiogenesis, Zebrafish

INTRODUCTION

Endothelial cells (ECs) undergo rapid changes in cellular morphology during blood vessel morphogenesis, a process that involves migration, cell division, establishment of polarity and cell junctions, cell intercalation and lumen formation. Thus, the cell body has to be flexible yet retain sufficient strength to maintain structural integrity (Kapustina et al., 2013). The actin cytoskeleton is integral in providing cells with mechanical support and driving forces for movement (Pollard and Cooper, 2009). Filamentous actin (F-actin) can assemble into distinct cellular structures, such as filopodia and lamellipodia, that confer the capacity to migrate (Chhabra and Higgs, 2007). In addition, the actin cytoskeleton provides anchorage to the extracellular matrix through focal adhesions and to neighbouring cells through adherens junctions (Bayless and Johnson, 2011). The cytoskeleton therefore senses both external forces applied to the cell and the mechanical properties of the cell's environment (Pollard and Cooper, 2009).

During sprouting angiogenesis *in vivo*, endothelial tip cells extend many filopodia that show polarity towards the direction of migration (Gerhardt et al., 2003). The classical view of filopodia is that they act as antennae to probe the extracellular environment for guidance cues, matrix composition and the presence of other cells (Mattila and Lappalainen, 2008; Mellor, 2010; Arjonen et al., 2011). It is therefore assumed that filopodia mediate endothelial tip cell migration to guide vascular sprout formation and vascular patterning. However, the function of filopodia in guided EC migration *in vivo* has not been directly examined.

Our current knowledge of actin cytoskeleton formation, organisation and rearrangement during angiogenesis and how it influences EC behaviour is limited to *in vitro* studies, in which cells have been removed from their physiological environment and lack features such as blood flow, extracellular matrix and mechanical input from surrounding tissue. Recent developments in actin probes have led to the generation of animal models expressing the F-actin reporter Lifeact (Riedl et al., 2008; Riedl et al., 2010; Yoo et al., 2010; Fraccaroli et al., 2012), allowing visualisation of actin-based structures in cells *in vivo*. Analysis of postnatal mouse retinal ECs using Lifeact-EGFP reporter mice showed localisation of F-actin at various intracellular compartments, such as cell-cell junctions, apical and basal membranes and filopodia (Fraccaroli et al., 2012). Although this study provides insight into endothelial F-actin organisation under physiological conditions, it does not provide temporal information on the formation and dynamics of F-actin owing to limitations of the mouse retina model of angiogenesis.

In the present study we sought to first visualise F-actin *in vivo* in order to characterise the dynamics of specialised intracellular actin-based structures. We generated a transgenic zebrafish line in which Lifeact, a 17 amino acid peptide from Abp140 that binds to F-actin (Riedl et al., 2008), fused to enhanced green fluorescent protein (Lifeact-EGFP) is expressed in ECs. By live imaging, we are able to examine the dynamics of F-actin in various angiogenic processes such as migration, proliferation and establishment of cell junctions. We next addressed the functional importance of filopodia in sprouting angiogenesis *in vivo* by inhibiting endothelial filopodia formation with low concentrations of Latrunculin B. Interestingly, we discovered that endothelial filopodia are dispensable for tip cell induction and guidance but facilitate anastomosis as well as rapid and persistent EC migration.

[1]KU Leuven, Department of Oncology, Vesalius Research Centre, Vascular Patterning Lab, Herestraat 49, 3000 Leuven, Belgium. [2]VIB, Vesalius Research Centre, Vascular Patterning Lab, Herestraat 49, 3000 Leuven, Belgium. [3]Vascular Biology Laboratory, London Research Institute, Cancer Research UK, 44 Lincoln's Inn Fields, London WC2A 3LY, UK.

*Authors for correspondence (likun.phng@vib-kuleuven.be; holger.gerhardt@cancer.org.uk)

MATERIALS AND METHODS

Zebrafish strains

Zebrafish (*Danio rerio*) were raised and staged as previously described (Kimmel et al., 1995). The following transgenic lines were used: *Tg(Fli:GFP)*[y1] (Lawson and Weinstein, 2002), *Tg(Fli:nEGFP)*[y7] (Roman et al., 2002) and *Tg(Kdr-l:ras-Cherry)*[s916] (Hogan et al., 2009a).

Cloning, constructs and transgenic line generation

All constructs were generated using the Tol2Kit (Kwan et al., 2007) and the three-insert Multisite Gateway system (Invitrogen). A Lifeact (Riedl et al., 2008) middle entry clone (pME-Lifeact) and human ZO-1 (pEGFP-C1 ZO1 was a gift from Markus Affolter, University of Basel, Switzerland) 3′ entry clone (p3E-ZO-1) were generated by BP reactions. For endothelial specific expression, the *Fli1ep* promoter (p5E-Fli1ep, a gift from Nathan Lawson, University of Massachusetts Medical School, USA) was used to drive the expression of Lifeact-EGFP and mCherry-ZO1 fusion constructs. One-cell stage embryos were injected with 25 ng/µl plasmid and 25 ng/µl Tol2 transposase RNA. Capped mRNAs were transcribed with the SP6 mMESSAGE mMACHINE Kit (Ambion). Embryos injected with pTol2-Fli1ep:Lifeact-EGFP were raised to adults and screened for founders.

Morpholino, heat-shock and pharmacological experiments

Standard control and *dll4* splicing (Leslie et al., 2007) antisense morpholinos (Gene Tools) were diluted in water containing Phenol Red. 15 ng oligonucleotide was injected into the yolk of 1- to 2-cell stage embryos. For ectopic expression of Vegfa165, pTolHSPVegfa165-IRES-nlsEGFP plasmid (gift from Nathan Lawson) was injected into 1-cell stage embryos. Embryos were heat shocked at 37°C for 30 minutes. Latrunculin B (Merck Millipore) was dissolved in DMSO to 1 mg/ml, stored at −20°C and diluted to the desired concentration in Danieau's Buffer containing 0.04% DMSO.

Imaging, image processing and statistical analysis

Live embryos were mounted in 0.8% low-melting agarose containing 0.01% Tricaine (Sigma) and bathed in Danieau's Buffer. Images and time-lapse movies were acquired using an Andor Revolution 500 spinning disk confocal built on a Nikon TiE inverted microscope equipped with an Andor iXon3 EMCCD camera and Yokogawa CSU-X1 spinning disk unit. z-stacks were captured at 1 µm intervals and flattened by maximum projection unless otherwise stated. Image processing, measurements, kymographs, stitching (Preibisch et al., 2009) and tracking were performed using ImageJ 1.47j software. To measure cortical F-actin expression, the mean Lifeact-EGFP fluorescence intensity within a region of interest (ROI) at the cell cortex was measured. *xy* drifts were corrected using the StackReg Translation plug-in (Thévenaz et al., 1998) before tracking using the Manual Tracking plug-in. Statistical analyses were performed using a two-tailed Student's *t*-test in Prism 5.0 (GraphPad); *P*≤0.05 was considered statistically significant.

RESULTS

Generation of an endothelial Lifeact transgenic line to examine F-actin dynamics *in vivo*

To investigate actin cytoskeleton dynamics and their role in angiogenesis *in vivo*, we generated a transgenic zebrafish line that expresses the small F-actin-binding peptide Lifeact (Riedl et al., 2008) in ECs. Lifeact was tagged with EGFP at the C-terminus and its expression was driven by the endothelial *Fli1ep* promoter. Injected fish were raised to adulthood and screened for germline transmission of the transgene. Embryos from *Tg(Fli1ep:Lifeact-EGFP)* fish display Lifeact-EGFP expression in the ECs of many vascular segments, such as the arterial, venous and lymphatic intersomitic vessels (ISVs), the vein plexus, branchial arches, hindbrain vasculature and subintestinal vessels (supplementary material Fig. S1A-H). However, weak Lifeact-EGFP expression is also observed in some non-ECs, including muscle fibres of the myotome, macrophages, neurons and lateral line primordium. Staining of *Tg(Fli1ep:Lifeact-EGFP)* embryos with the F-actin marker phalloidin showed colocalisation of Lifeact with phalloidin

in ECs of the ISV (supplementary material Fig. S1I,J), thus confirming Lifeact as an F-actin marker *in vivo*.

Dynamic F-actin polymerisation in migrating ECs

By performing live imaging of developing ISVs in *Tg(Fli1ep:Lifeact-EGFP)* embryos, we detected F-actin in various subcellular structures, including filopodia (Fig. 1A-C), cell cortex (Fig. 1A,B) and in clusters within the plasma membrane and the cytoplasm (Fig. 1C). Prominent F-actin clusters are frequently detected at the migrating front of vascular sprouts and at the base of filopodia (Fig. 1A). In actively sprouting ECs, cortical F-actin formation is heterogeneous and dynamic within a cell. This is illustrated in Fig. 1B, which shows a single cell expressing Lifeact-EGFP spanning the ISV and dorsal longitudinal anastomotic vessel (DLAV). The presence of cortical F-actin at the neck of the T-shaped cell (Fig. 1B) correlates with a tenser cell cortex (Salbreux et al., 2012), compared with the region ventral to the neck that is devoid of cortical actin, where the cell cortex appears more relaxed.

Dynamic changes in F-actin polymerisation at different subcellular structures were also observed during cell proliferation. One hour prior to cell division, there is a gradual increase in cortical F-actin, as indicated by an increase in Lifeact-EGFP intensity that peaks just before cytokinesis and decreases after its completion (Fig. 1D,E). Conversely, there is an 85% decrease in F-actin-positive filopodia at the onset of cytokinesis compared with 39 minutes earlier (Fig. 1F). This decrease is transient, as upon completion of cytokinesis there is a resurgence in the number of filopodia protrusions. We also detected an increase in F-actin-rich membrane blebs (Fig. 1D; supplementary material Movie 1), which dissipated at the onset of cytokinesis, and an enrichment of F-actin at the cleavage furrow, where it forms the contractile ring (Fig. 1D).

As vessel sprouts become multicellular, F-actin polymerises at cell junctions (Fig. 1C, Fig. 2). We confirmed this by co-expressing Lifeact-EGFP with human zona occludens 1 (also known as tight junction protein 1), a tight junction molecule, fused to mCherry (mCherry-ZO1) in ECs (Herwig et al., 2011). Lifeact and ZO1 colocalise in the developing longitudinal junctions of ISVs of embryos at 31 hours postfertilisation (hpf) (Fig. 2A″), in ring-shaped junctions formed by two ECs at the DLAV (supplementary material Fig. S2), and in the developed ISVs at 3 (supplementary material Fig. S1H) and 4 (Fig. 2B) days postfertilisation (dpf). ZO1 was also detected in some punctate F-actin structures in endothelial sprouts (Fig. 2A′), suggesting that F-actin and ZO1 share a non-junctional compartment in tip cells that could potentially contribute to newly forming junctions.

To characterise F-actin polymerisation in filopodia further, we compared the localisation of Lifeact-EGFP with that of a membrane marker by crossing *Tg(Fli1ep:Lifeact-EGFP)* fish with *Tg(Kdr-l:ras-Cherry)*[s916] fish, in which mCherry is tagged with the membrane-localising sequence of Ras that includes the CAAX motif (mCherryCAAX) (Wright and Philips, 2006). We discovered that although F-actin polymerisation is prominent in filopodia (Figs 1, 2), F-actin does not always span the whole length of the filopodium as highlighted by mCherryCAAX (Fig. 3A-E). F-actin length, from the base to the tip, varied among filopodia (Fig. 3F). In an analysis in which 108 filopodia were examined, 2.3% of filopodia did not exhibit Lifeact signal, 17.6% showed Lifeact signal through the entire filopodium, and 23.1%, as the largest fraction of the filopodia, displayed Lifeact signal 90% of the length of the filopodium. The variation in F-actin polymerisation among filopodia might be due to limitations in detectable Lifeact-EGFP signal, which may lead to reduced measurement of F-actin in
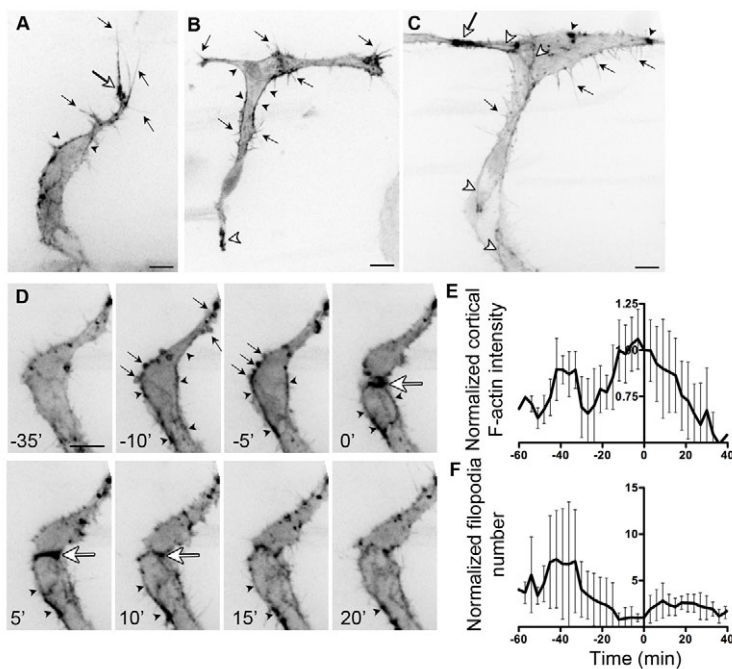
Fig. 1. F-actin localisation in endothelial cells during angiogenesis. (**A**) Migrating intersomitic vessel (ISV) from a 32 hpf *Tg(Fli1ep:Lifeact-EGFP)* zebrafish embryo. F-actin is prominent in filopodia (black arrows), the base of filopodia (white arrow) and cell cortex (arrowheads). (**B**) Single-cell expression of Lifeact-EGFP in an endothelial cell (EC) spanning the ISV and dorsal longitudinal anastomotic vessel (DLAV) at 31 hpf. Cortical F-actin (black arrowhead) is present at the neck of the cell. Arrows indicate filopodia. White arrowhead points to enrichment of F-actin at the ventral end of the cell. (**C**) During anastomosis of ECs at the DLAV, there is enrichment of F-actin at points of contact (white arrow). F-actin is also found at cell junctions (white arrowheads), filopodia (black arrows) and in punctate structures (black arrowheads). (**D**) Still images of a time-lapse movie of ISV from a 31 hpf *Tg(Fli1ep:Lifeact-EGFP)* embryo undergoing cell division. Arrows point to F-actin-rich membrane blebs prior to cell division (−10 and −5 minutes). Arrowheads indicate accumulation of cortical actin. Strong accumulation of F-actin is observed at the contractile ring (white arrow) during cytokinesis. (**E,F**) Normalised cortical F-actin intensity (E) and filopodia number (F) before, during and after cell division. Raw values were normalised to the value at 0 minutes, at which two daughter cells are observed. Mean ± s.d. *n*=5 cells. Scale bars: 10 μm.

filopodia. Alternatively, this might be a reflection of the dynamic nature of F-actin polymerisation within the filopodium. Filopodial protrusions and retractions are determined by the balance between actin polymerisation at the barbed ends of a filament and the retrograde flow of the actin filament bundle (Mattila and Lappalainen, 2008). A shorter Lifeact length might indicate a decreased F-actin polymerisation rate that precedes filopodia retraction (supplementary material Fig. S3A). However, we also observed examples in which shortening of F-actin does not lead to retraction of filopodia (supplementary material Fig. S3B). Thus, the observation of different F-actin filament lengths might be a result of the net effect of actin polymerisation regulators with activities that vary between filopodia and during different phases of filopodia lifetime.

Live imaging of F-actin-positive filopodia revealed that one or two filopodia become dominant during ISV development (Fig. 3G; supplementary material Movie 2). We frequently observed transient bursts of F-actin-rich lamellipodia-like protrusions that emanated laterally from stable filopodia for 30 to 45 minutes. This was followed by rapid lateral expansion of the filopodium (Fig. 3G), leading to an increase in vessel width and coverage.

Low concentrations of Latrunculin B inhibit F-actin polymerisation in filopodia

To further confirm the specificity of Lifeact-EGFP as a marker for F-actin as well as to study the role of F-actin in EC biology during angiogenesis *in vivo*, we treated *Tg(Fli1ep:Lifeact-EGFP)* embryos with Latrunculin B (Lat. B), a toxin that binds to actin monomers and prevents polymerisation (Morton et al., 2000). Twenty minutes after the addition of 2 μg/ml Lat. B, developing ISVs still exhibit F-actin in filopodia and at the cell cortex and junctions (supplementary material Fig. S4A). As treatment continued, there is a progressive loss of F-actin in filopodia (supplementary material Fig. S4B-E, 65 to 230 minutes post-treatment) and an increase in Lifeact-EGFP puncta in the cytoplasm (supplementary material Fig. S4B-D, 65 to 230 minutes), followed by a loss of junctional F-actin and a concomitant increase in EGFP signal in the cytoplasm

(supplementary material Fig. S4D, 230 minutes). The disruption of F-actin polymerisation also led to a perturbation in cell morphology. The first noticeable change was the retraction of existing filopodia and the inhibition of new filopodia formation. This was followed by changes in cell morphology; cell shape and protrusions appeared more convoluted after 230 minutes of 2 μg/ml Lat. B treatment.

As long-term treatment with high concentrations of Lat. B leads to embryonic lethality, we determined the concentration of the drug that leads to disruption of endothelial actin polymerisation without affecting myocardial contraction or survival. Early embryos treated with 0.15 μg/ml Lat. B from 30 hpf survive 17 hours of treatment, with a strong heart beat visible at 47 hpf (100% survival, *n*=26). Embryos begin to show vulnerability when treated with 0.2 μg/ml Lat. B (85% survival, *n*=27), with surviving embryos appearing smaller with kinked tails and a slower heart rate. We therefore proceeded to use concentrations of 0.15 μg/ml Lat. B and below in subsequent experiments.

Although junctional F-actin is present after 5 hours of treatment with 0.15 μg/ml Lat. B, migrating ISVs show a loss of filopodia protrusions (Fig. 4B) compared with control embryos, which exhibit abundant F-actin- and mCherryCAAX-positive filopodia (Fig. 4A). Lower concentrations of Lat. B (0.08 to 0.1 μg/ml) also inhibit filopodia formation (Fig. 4D,F, Fig. 5N, Fig. 7B,D). Tip cells of control embryos protrude many filopodia that make connections with each other when 15-20 μm apart to form the future DLAV (Fig. 4C). In tip cells that lack filopodia, such contacts are not observed at this distance apart (Fig. 4D). Similarly, treatment with 0.1 μg/ml Lat. B led to a loss of filopodia by ECs at the vein plexus (Fig. 4F), as compared with DMSO-treated embryos (Fig. 4E). Treatment with low concentration of Lat. B also revealed a change in the F-actin structure assembled; there is a decrease in F-actin bundles but an increase in F-actin clusters (Fig. 4B,D,F).

These experiments revealed that it is possible to use low concentrations of Lat. B, of between 0.08 and 0.1 μg/ml and referred to as low Lat. B hereafter, to dissect the function of filopodia during sprouting angiogenesis.
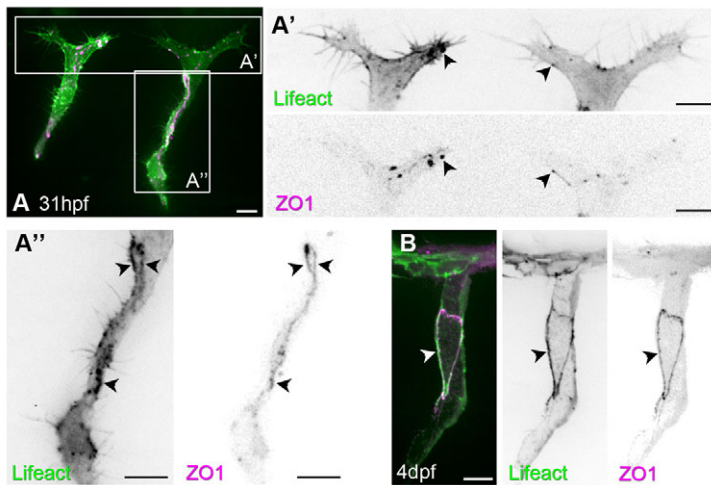
Fig. 2. F-actin polymerises at cell junctions. (**A-B**) Clonal expression of Lifeact-EGFP and mCherry-ZO1 in ISVs. Arrowheads indicate colocalisation of F-actin and ZO1 in puncta (A', single plane of endothelial tip cell) and cell junctions (A",B). Scale bars: 10 µm.

## Filopodia are dispensable for endothelial tip cell guidance

Filopodia have been ascribed sensory or exploratory functions as their long projections probe the cell's surroundings and act as a site for signal transduction (Faix and Rottner, 2006; Mattila and Lappalainen, 2008). Time-lapse imaging of zebrafish ISV development reveals dorsal migration of endothelial tip cells, from the axial dorsal aorta (DA) at somite boundaries to the dorsal roof of the neural tube, where they extend protrusions rostrally and caudally to form the DLAV (Isogai et al., 2003). As migration of tip cells is stereotypic and directed, we consider their migration to be guided. Migration of ECs is regulated by the combined activities of proangiogenic cues such as Vegf signalling (Covassin et al., 2006; Hogan et al., 2009b; Krueger et al., 2011) and repulsive cues such as Ephrin B/EphB4 (Helbling et al., 2000), Netrin 1/Unc5b (Lu et al., 2004) and Semaphorin/Plexin D1 (Childs et al., 2002; Torres-Vázquez et al., 2004) signalling. We therefore examined whether filopodia are essential for the guided migration of ECs during ISV and DLAV formation in the zebrafish trunk.

We treated embryos with low Lat. B from 24 hpf, when ISVs posterior to the yolk sac extension have emerged from the DA and start to migrate dorsally. At 48.5 hpf, treated embryos (Fig. 5B) appear smaller than control embryos (Fig. 5A) but show a heartbeat. Analysis of ISVs between the end of the yolk sac extension and the tail revealed the migration of ISVs along the normal trajectory. The length of ISVs at positions 1 to 10 is similar in control and Lat. B-treated embryos, whereas a significant decrease is observed at positions 11 to 15, which are most distal from the yolk extension where ISVs are formed later (Fig. 5C). There is also a 34.5% decrease in the number of connected DLAV segments (Fig. 5D) in embryos treated with low Lat. B compared with control embryos at 48.5 hpf, with most of the unconnected DLAV segments located at the posterior end of the embryo. These data suggest that ECs are able to migrate in the absence of filopodia but at a decreased velocity, resulting in a delay in ISV migration and DLAV formation. This is supported by time-lapse imaging, which shows correct pathfinding by ISVs in the presence of low Lat. B (Fig. 5H,I; supplementary material Movies 3,7). Kymographs of ISV migration from embryos treated with low Lat. B show that the lack of filopodia correlates with a slower and staggered migration (Fig. 5J) compared with embryos treated with DMSO (Fig. 5G). By tracking the migrating front of ISV sprouts above the horizontal myoseptum, we observed that ISVs lacking filopodia migrate 49% slower than ISVs

with filopodia (DMSO, 0.196±0.30 µm/minute; Lat. B, 0.099±0.056 µm/minute; Fig. 5K). Similar results were also obtained by tracking nuclei of tip cells. During ISV growth, tip cells display differences in velocity when migrating below
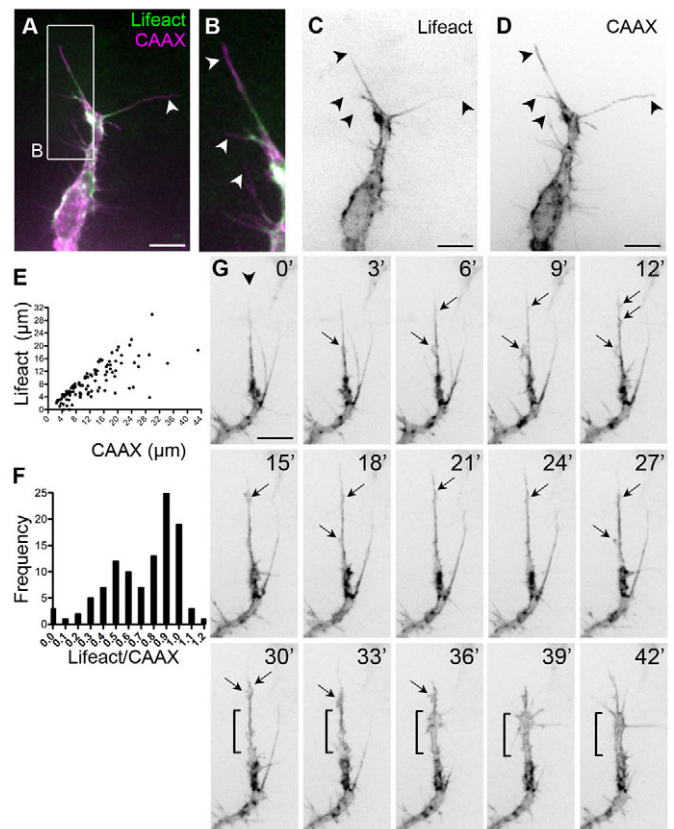
Fig. 3. Dynamic F-actin localisation in filopodia. (**A-D**) Sprouting front of an ISV from a 30 hpf *Tg(Fli1ep:Lifeact-EGFP); Tg(Kdr-l:ras-Cherry)[s916]* zebrafish embryo. Arrowheads indicate filopodia. (**E**) Length of the Lifeact signal in a CAAX-labelled filopodium. *n*=108 filopodia. (**F**) Frequency distribution of Lifeact/CAAX filopodia length. *n*=108 filopodia. (**G**) Dynamics of F-actin in a sprouting ISV from *Tg(Fli1ep:Lifeact-EGFP)* embryos. Lamellipodia-like structures (arrows) emanate from the most persistent filopodium (arrowhead) and give rise to a rapid expansion in vessel volume (from 30 to 42 minutes, bracket). Scale bars: 10 µm.
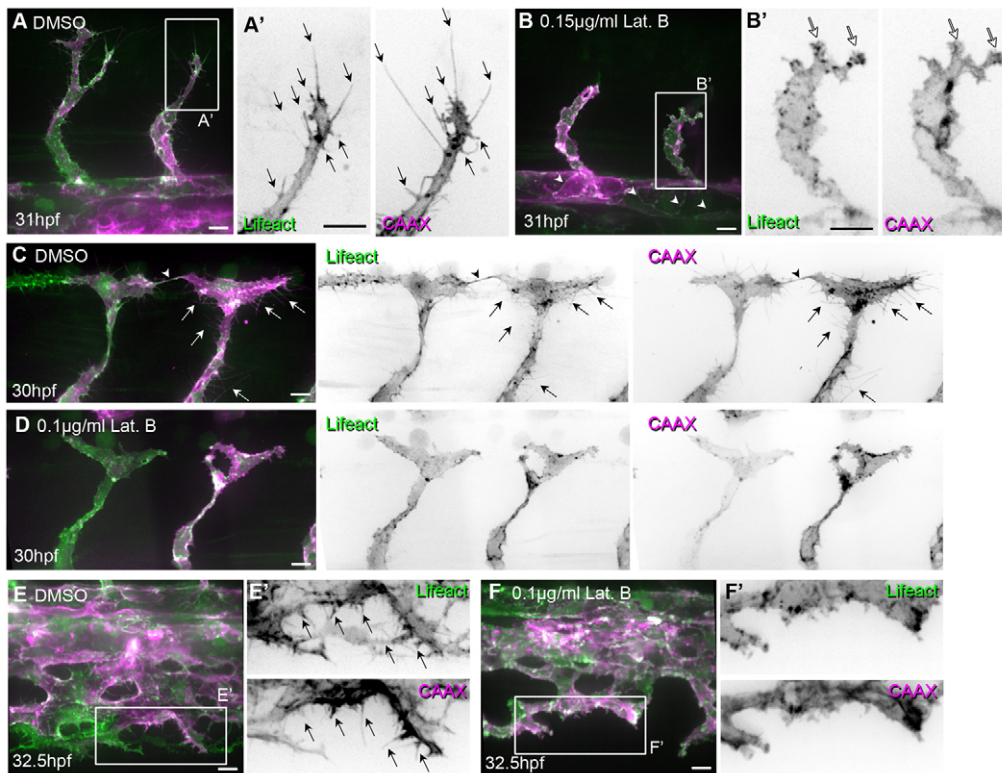
Fig. 4. Low concentrations of Latrunculin B inhibit filopodia formation. *Tg(Fli1ep:Lifeact-EGFP); Tg(Kdr-l:ras-Cherry)^{ss916}* zebrafish embryos were treated with 0.4% DMSO (control) or low concentrations of Latrunculin B (Lat. B) from (**A-B′**) 24 to 29 hpf, (**C-D′**) 26 to 29 hpf or (**E-F′**) 26.5 to 32 hpf. (A-B′) Arrows highlight filopodia on sprouting ISVs. White arrows indicate lamellipodia-like protrusions. Arrowheads point to junctional F-actin at dorsal aorta. (C-D′) Arrows indicate filopodia. Arrowhead highlights filopodia-based contacts between two tip cells that form the DLAV. (E-F′) Arrows indicate filopodia at vein plexus. Scale bars: 10 μm.

(0.198±0.167 μm/minute), at (0.139±0.220 μm/minute) and above (0.189±0.261 μm/minute) the horizontal myoseptum (Fig. 5L; supplementary material Fig. S5A,B, Movie 4). In embryos treated with low Lat. B, tip cell nuclei migrate significantly slower at (0.155±0.013 versus 0.0930±0.008 μm/minute for DMSO versus Lat. B; *P*=0.0009) and above (0.203±0.027 versus 0.077±0.013 μm/minute for DMSO versus Lat. B; *P*=0.0018) the horizontal myoseptum compared with control embryos (Fig. 5L).

As cell division is an actin-driven process, we examined whether EC proliferation is perturbed with low Lat. B treatment. Analysis of time-lapse videos revealed a similar increase in EC number during ISV growth between DMSO- and Lat. B-treated embryos within a 13.5-hour period: 2.133±0.306 and 2.117±0.333 cells/ISV (*P*=0.9521), respectively. In DMSO-treated embryos, 51.9% of new ECs arise from cell division, whereas in low Lat. B-treated embryos 40.1% arise from division (Fig. 5M). EC migration from the DA contributes to the remaining increase in cell number. Although there is an 11.8% decrease in cell division, this difference is small and insignificant (*P*=0.6129), indicating that short-term treatment with low concentrations of Lat. B does not significantly perturb EC proliferation in ISVs.

Detailed analyses of the sprouting front of ISVs revealed that endothelial tip cells are able to generate lamellipodia in the direction of migration in the absence of filopodia (Fig. 5N; supplementary material Movie 5). In addition, clusters of F-actin polymerise at the leading edge of the tip cell, possibly driving lamellipodia formation (Fig. 5N). These observations suggest that, in the absence of filopodia, lamellipodia formation is sufficient for reading guidance cues and to generate the force required for migration.

Filopodia are not required for endothelial tip cell selection and ectopic sprouting

Notch signalling is essential in regulating endothelial tip cell selection and vessel branching (Phng and Gerhardt, 2009). In zebrafish embryos, knockdown of the endothelial Notch ligand Delta-like 4 (Dll4) leads to an increase in tip cell formation and ectopic branching at ISVs and DLAVs (Leslie et al., 2007; Siekmann and Lawson, 2007). We examined whether filopodia are essential for the formation of tip cells upon inhibition of Dll4 signalling. At 49 hpf, control morphants treated with DMSO display a network of DLAVs with secondary sprouts (Fig. 6A) that is not observed in embryos treated with low Lat. B from 30 hpf (Fig. 6D) due to a delay in anastomosis. Embryos injected with Dll4 splice morpholino showed increased vessel branching at the DLAV and ectopic sprouting from the ISVs (Fig. 6B,C), as shown previously (Leslie et al., 2007). Similarly, Dll4 morphants treated with low Lat. B from 30 hpf displayed ectopic sprouting from the DLAV even in the absence of filopodia (Fig. 6E,F), indicating that filopodia are not essential for tip cell formation and ectopic branching.

The patterning of the zebrafish trunk vasculature is tightly coordinated by Vegf, Semaphorin/Plexin D1 and Netrin 1/Unc5b signalling (Childs et al., 2002; Lu et al., 2004; Torres-Vázquez et al., 2004; Covassin et al., 2006; Hogan et al., 2009b; Krueger et al., 2011). We examined whether ECs without filopodia respond to changes in guidance cues by expressing Vegfa165 (Vascular endothelial growth factor A isoform 165) randomly in the embryo at various developmental stages. We injected plasmid encoding Vegfa165-IRES-nuclear EGFP under the heat-shock promoter into 1-cell stage embryos and induced Vegfa165 expression either before or after completion of ISV formation. Embryos were subsequently treated with DMSO or low Lat. B and examined 1 day later. Uninjected, heat-shocked and DMSO-treated embryos showed normal ISV and DLAV patterning at 47 and 76 hpf (Fig. 6G,J). However, mispatterning was observed in embryos in which ectopic Vegfa165 is expressed by cells in close proximity to ISVs, as revealed by nuclear EGFP expression (Fig. 6H,I,K-O). When Vegfa165 expression was induced before ISV and DLAV formation
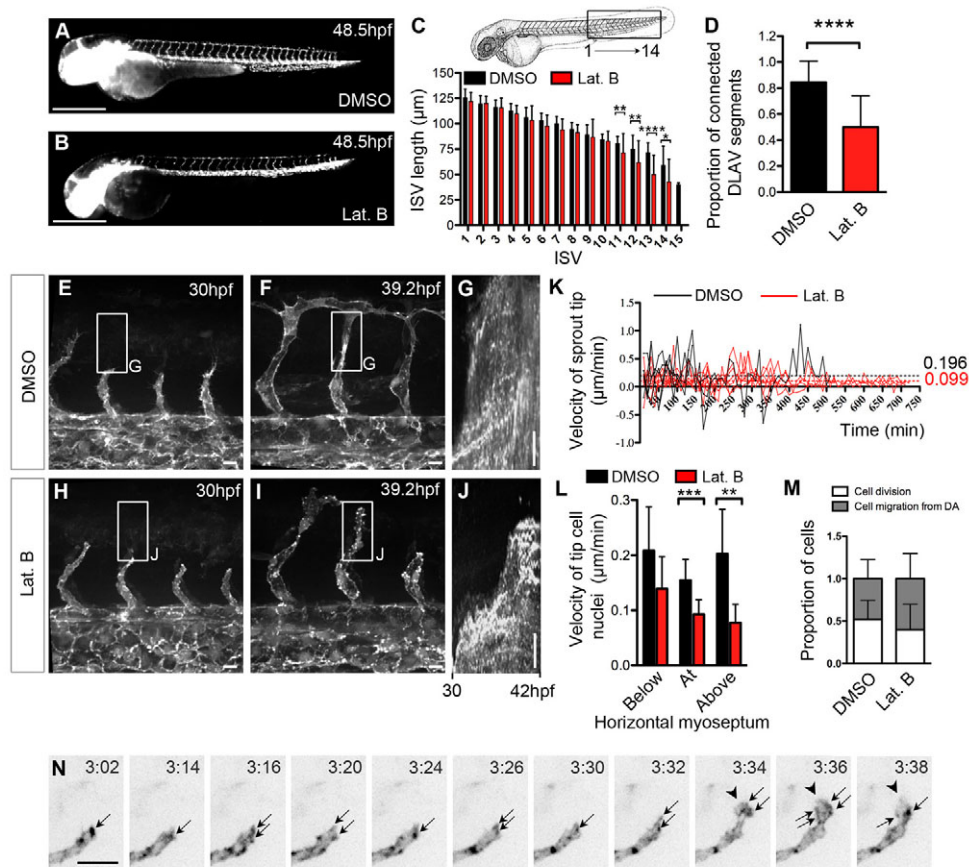
Fig. 5. Absence of filopodia decreases migration velocity but does not affect guided migration. (**A-D**) *Tg(Fli:GFP)^{y1}* zebrafish embryos treated with 0.4% DMSO (A) or 0.08 μg/ml Lat. B (B) from 24 to 47.5 hpf. (C) Length of ISVs between the yolk end and tail at 48.5 hpf. DMSO, *n*=44 embryos; Lat. B, *n*=39 embryos. (D) Proportion of connected DLAV segments per embryo at 48.5 hpf. DMSO, *n*=43 embryos; Lat. B, *n*=38 embryos. (**E-K**) *Tg(Fli1ep:Lifeact-EGFP)* embryos treated with either 0.4% DMSO (E,F) or 0.1 μg/ml Lat. B (H-J) from 24 hpf and imaged from 30 hpf. (G,J) Kymographs of ISVs in E and H (boxed regions) showing migration from 30 to 42 hpf. (K) Leading edge velocity of ISVs migrating above the horizontal myoseptum. Dotted lines indicate mean velocities. Negative values indicate sprout retraction. DMSO, *n*=5 ISVs, *n*=2 embryos; 0.1 μg/ml Lat. B, *n*=8 ISVs, *n*=3 embryos. (**L**) Average tip cell nucleus velocity per ISV below, at and above the horizontal myoseptum of embryos treated with 0.4% DMSO or 0.1 μg/ml Lat. B. DMSO, *n*=7-9 nuclei, *n*=3 embryos; 0.1 μg/ml Lat. B, *n*=7-10 nuclei, *n*=3 embryos. (**M**) Proportion of ECs that arise from cell division and migration from the dorsal aorta during 13.5 hours of ISV development in DMSO-treated and 0.1 μg/ml Lat. B-treated embryos. 14-15 ISVs/treatment; three embryos/treatment. (**N**) Migrating front of an ISV from a *Tg(Fli1ep:Lifeact-EGFP)* embryo treated with 0.08 μg/ml Lat. B from 26 hpf. Arrows point to clusters of F-actin formed at the leading edge of the tip cell. Arrowheads indicate lamellipodia. Time indicates hours:minutes after addition of the drug. *P<0.05, **P<0.005, ***P<0.001, ****P<0.0001. Error bars represent s.d. Scale bars: 500 μm in A,B; 10 μm in E-J,N.

was completed, we observed ectopic branching between ISVs at the horizontal myoseptum and an increased number of branches connecting ISVs to the DLAV, thereby indicating misguidance of EC migration during development. This phenotype was observed in embryos treated with DMSO (Fig. 6H) as well as with low Lat. B (Fig. 6I), demonstrating that ECs lacking filopodia can also respond to changes in guidance cues in the surrounding tissue to a similar extent to cells with filopodia. Vegfa165-induced ectopic branching can also be initiated after completion of ISV formation. Embryos treated with DMSO or low Lat. B show ectopic branching (Fig. 6K,L) from the ISV towards sources of Vegfa165. Time-lapse imaging provided further evidence of vessel misguidance (supplementary material Movie 6) and ectopic sprout formation from the ISV and the DA in the absence of filopodia (Fig. 6M; supplementary material Movie 6). In another example, ectopic branches were observed to emanate from the ISV and cardinal vein towards a cell expressing high Vegfa165 to form a disorganised vessel network (Fig. 6N,O).

These findings provide further proof that ECs do not depend on filopodia to receive guidance cues and to direct blood vessel migration.

Filopodia facilitate blood vessel anastomosis

Our observations also indicate a role of filopodia in facilitating vessel anastomosis, as their absence delayed DLAV formation and blocked vein plexus formation. In control embryos, endothelial tip cells of ISVs project multiple filopodia rostrally and caudally when they reach the dorsal roof of the neural tube (Fig. 7A, 0 minutes). Filopodia of neighbouring cells interact (Fig. 7A, 27 minutes) and form a stable site of contact (Blum et al., 2008; Herwig et al., 2011), where F-actin polymerisation is prominent, within 2 hours (Fig. 7A). However, such efficient contact formation between two tip cells is not observed when ECs are depleted of filopodia (Fig. 7B). ISVs of embryos treated with low Lat. B can branch at the dorsal roof of the neural tube (Fig. 7B, 0 minutes) but are unable to establish contact and initiate DLAV formation within 2 hours
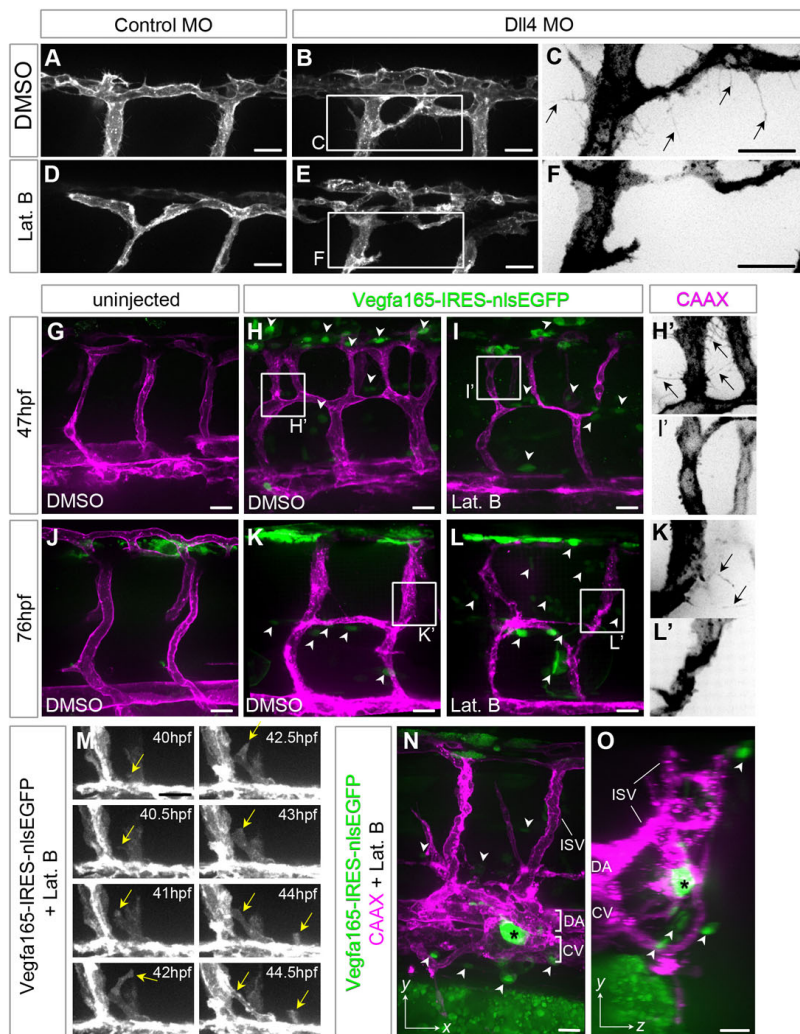
Fig. 6. Endothelial tip cell selection and ectopic sprouting occur in the absence of filopodia.
(**A-F**) *Tg(Kdr-l:ras-Cherry)^s916* zebrafish embryos injected with 15 ng control or Dll4 morpholino, treated with either 0.4% DMSO or 0.08 µg/ml Lat. B from 30 hpf and imaged at 49 hpf. (**G-O**) *Tg(Kdr-l:ras-Cherry)^s916* embryos injected with HSP:Vegfa165-IRES-nlsEGFP plasmid. (G-I',M) Uninjected and injected embryos were heat shocked at 24 hpf, treated with 0.4% DMSO or 0.08 µg/ml Lat. B from 29 hpf, and examined at 47 hpf. (J-L',N,O) Uninjected and injected embryos were heat shocked at 51 hpf, treated with 0.4% DMSO or 0.1 µg/ml Lat. B at 52 hpf, and examined at 76 hpf. Arrowheads indicate cells expressing nuclear EGFP and Vegfa165. Arrows highlight filopodia. Yellow arrows indicate ectopic sprout from the dorsal aorta. Asterisk indicates a cell expressing high levels of Vegfa165. DA, dorsal aorta; CV, caudal vein; ISV, intersomitic vessel. Scale bars: 20 µm.

(Fig. 7B, 117 minutes). DLAV formation can still proceed, as DLAV formation between ISVs was observed during live imaging albeit fewer in number (Fig. 5B,D; supplementary material Movie 7).

Inhibition of endothelial filopodia formation at the vein plexus also stalled the progress of vein plexus formation. Treatment with low Lat. B from 31 hpf resulted in incomplete formation of dorsal and ventral vein plexus at 47 hpf compared with DMSO-treated embryos (Fig. 7C,D; supplementary material Movie 7). Unlike ECs of the ISVs, cells at the vein plexus do not adopt a lamellipodial form of migration once filopodia formation is inhibited. Instead, sprouts become globular in shape and the vessel network remained unfused and immature (supplementary material Fig. S6B).

The above results reveal the exploratory role of filopodia in facilitating encounters with neighbouring endothelial tip cells and show that this process is important in blood vessel anastomosis.

DISCUSSION
Tg(Fli1ep:Lifeact-EGFP) enables visualisation of blood vessel architecture with cellular detail
By using *Tg(Fli1ep:Lifeact-EGFP)* transgenic embryos and time-lapse light microscopy, we show that F-actin polymerisation is dynamic and assembles different subcellular structures in ECs during angiogenesis. We observed two types of F-actin structures: (1) F-actin bundles that form at the cell cortex, cell junctions, in filopodia and contractile ring; and (2) F-actin clusters that assemble

at the migrating front of vessel sprouts, base of filopodia and in the cytoplasm. Furthermore, time-lapse imaging revealed F-actin structures that are transient, such as filopodia, contractile ring and cortical F-actin, and more persistent structures, such as junctional F-actin. These observations suggest that the turnover rate of actin polymerisation is different and highly regulated in distinct intracellular compartments.

Experiments with the actin polymerisation inhibitor Lat. B suggest that F-actin bundles and clusters have different properties, as they are differentially affected by the drug. Treatment with high concentrations of Lat. B leads to a progressive loss of F-actin-based structures. The first structure to disappear is filopodia, followed by disintegration of cortical and junctional actin. Under low Lat. B conditions, the formation of F-actin bundles is compromised and we instead observe an increase in F-actin clusters that appears sufficient to drive EC migration, lumenisation and cell division.

Low concentrations of Latrunculin B inhibit filopodia formation by ECs
In our attempt to characterise F-actin behaviour in ECs, we discovered a method to inhibit filopodia formation using low concentrations of Lat. B. At concentrations between 0.08 and 0.15 µg/ml, we were able to selectively prevent filopodia formation without inhibiting other cellular processes such as contractile ring formation (supplementary material Movie 5, 222 minutes),
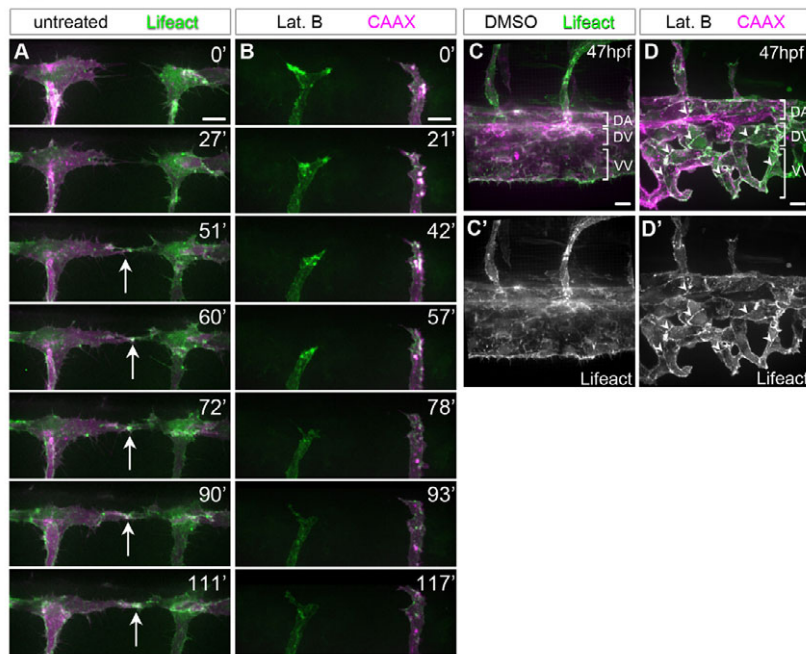
Fig. 7. Filopodia facilitate anastomosis of DLAV and the vein plexus. (A,B) Endothelial tip cells of untreated (A) and 0.08 µg/ml Lat. B-treated (B) 31 hpf *Tg(Fli1ep:Lifeact-EGFP); Tg(Kdr-l:ras-Cherry)^{s916}* zebrafish embryos at the dorsal roof of the neural tube. Arrows indicate polymerisation of F-actin at new cell contacts. Time is in minutes. **(C-D')** Vein plexi of *Tg(Fli1ep:Lifeact-EGFP); Tg(Kdr-l:ras-Cherry)^{s916}* embryos treated with DMSO or 0.1 µg/ml Lat. B from 31 to 46 hpf. Arrowheads indicate junctional F-actin. DA, dorsal aorta; DV, dorsal vein; VV, ventral vein. Scale bars: 10 µm.

junctional maintenance (Fig. 7D), EC division (Fig. 5M; supplementary material Movie 4) and vessel lumenisation (supplementary material Movie 7). Furthermore, we detected the migration of posterior lateral line primordium (data not shown) and macrophages (supplementary material Movie 7) at low Lat. B, indicating that the migratory activity of other cell types and tissues is uninhibited. Interestingly, low concentrations of Lat. B did not inhibit lamellipodia formation (Fig. 5N).

A possible explanation for the selectivity of low Lat. B is that a subsaturating level of the drug was used so that not all free actin monomers are bound and inhibited, leaving a population of free actin monomers available for residual F-actin polymerisation of structures such as the contractile ring and lamellipodia. As filopodia are highly dynamic structures with phases of elongation, stabilisation and persistence that are regulated by a balance between actin polymerisation and retrograde flow of the actin filament bundle (Mattila and Lappalainen, 2008; Schäfer et al., 2011), the formation of filopodia might be most sensitive to reduced levels of free actin monomers and become susceptible to inhibition by low Lat. B concentrations when other actin-based structures are not.

Filopodia are dispensable for EC migration and guidance

A similar method to inhibit filopodia formation has previously been reported in neuronal cells using low concentrations of the actin microfilament-disrupting agent cytochalasin B (Bentley and Toroian-Raymond, 1986; Chien et al., 1993; Zheng et al., 1996). However, unlike endothelial tip cells, neuronal growth cones require filopodia for chemotropic turning of cultured *Xenopus* spinal neurons (Zheng et al., 1996) and for correct pathfinding of *Schistocerca* Ti1 neurons (Bentley and Toroian-Raymond, 1986) and *Xenopus* retinal growth cones (Chien et al., 1993).

During sprouting angiogenesis, endothelial tip cells lead the path for vascular sprouts to invade tissues. In the zebrafish trunk, spatial organisation of the vasculature is regulated by Vegf (Covassin et al., 2006; Hogan et al., 2009b; Krueger et al., 2011), Netrin 1/Unc5B (Lu et al., 2004) and Semaphorin/Plexin D1 signalling (Childs et al., 2002; Torres-Vázquez et al., 2004), with the latter acting to

repress proangiogenic activities of Vegf signalling by ensuring expression of sFlt1 by ECs (Zygmunt et al., 2011). Perturbation of different components of these pathways affects angiogenesis and leads to mispatterning of the vasculature (Covassin et al., 2006; Hogan et al., 2009b; Krueger et al., 2011; Zygmunt et al., 2011). Thus, ECs receive and integrate a multitude of signals that aid their directed migration so as to enable the development of a stereotypic network of blood vessels with a reproducible pattern from animal to animal (Isogai et al., 2001; Isogai et al., 2003).

It is widely assumed that endothelial filopodia sense growth factors, extracellular matrix and guidance cues from the extracellular environment for correct vessel guidance and patterning (Gerhardt et al., 2003; De Smet et al., 2009; Adams and Eichmann, 2010; Ridley, 2011). Although it is possible that ECs receive guidance cues through activation of receptors present at filopodia, we discovered that filopodia are not essential for the guided migration of endothelial tip cells, as ISVs form in a stereotypic pattern in the complete absence of filopodia during embryonic development. This suggests that attractive and repulsive cues are received and integrated by ECs without filopodia. In addition, we demonstrated that ECs lacking filopodia are able to respond to ectopic Vegfa165 expression from cells located in the zebrafish trunk to form aberrant and misguided vessels. Repulsive cues, such as that provided by Sema3a secretion by somites, are not sufficient to prevent misguidance of ECs, suggesting that increased Vegfa signalling can override the repulsive effect of Sema3a-Plexin D1 signalling in ECs.

The lack of filopodia, however, resulted in decreased EC velocity, suggesting that although lamellipodia protrusion is sufficient for directional EC migration, filopodia facilitate the progress of migration. Filopodia have been described to emerge from lamellipodia, which act as a precursor structure (Biyasheva et al., 2004; Faix and Rottner, 2006). In this study, we show that filopodia can also serve as a precursor structure for lamellipodia-type protrusion (Fig. 3G; supplementary material Movie 2). Multiple lamellipodia can emanate along the length of a filopodium, permitting the rapid lateral expansion of vascular sprouts and increase in vessel area. Hence, in the absence of filopodia acting as a facilitator for vessel expansion, vessel growth occurs at a slower

rate and this might offer an explanation for the decrease in endothelial tip cell velocity and ISV length in the absence of filopodia.

Filopodia facilitate efficient blood vessel anastomosis

During dorsal closure in the *Drosophila* embryo, filopodia protrude from opposing cells to facilitate cell-cell matching and help epithelial sheets align and adhere together (Jacinto et al., 2000; Millard and Martin, 2008). Similarly, our data implicate the exploratory role of filopodia in increasing chance encounters with neighbouring tip cells to establish cell adhesion and vessel anastomosis. Furthermore, a previous study in macrophage-deficient PU.1 (*Spi1*) null mice suggests that the number of filopodia protrusions and the angular spread of filopodia at tip cells promote vessel anastomosis (Rymo et al., 2011).

We demonstrate in this study that the loss of filopodia has a significant effect on DLAV and vein plexus formation, although the latter vascular network appears more dependent on filopodia activity. Endothelial tip cells of the ISV are able to adopt a lamellipodia mode of migration in the absence of filopodia. Although lamellipodia appear sufficient for persistent migration, they are not as effective in the process of anastomosis, as loss of filopodia results in a 34.5% decrease in DLAV connections between ISVs. Lamellipodia, however, were not generated by ECs of the vein plexus after filopodia depletion. Movies of this region reveal that vascular sprouts in embryos subjected to low Lat. B fail to make vascular connections with neighbouring sprouts and that the plexus remains unfused. These data suggest that filopodia facilitate fusion and anastomosis of blood vessels and that ECs of different vascular plexi might have intrinsically different protrusive machinery. Notably, recent studies suggest that whereas ISV growth is Vegfa driven, sprouting from the axial vein is driven by Bmp signalling (Wiley et al., 2011; Kim et al., 2012). Thus, it is possible that the observed differences in lamellipodia formation and anastomosis are due to different intracellular mechanisms triggered by distinct growth factor stimuli. Finally, our results suggest that the process of anastomosis is not driven by chemotactic or haptotactic mechanisms but rather represents a contact-based process that requires the exploratory properties of filopodia.

ECs have the ability to generate different membrane protrusions

Cells have the ability to form different types of plasma membrane protrusions – filopodia, lamellipodia, invadopodia and blebs – in order to migrate through complex environments *in vivo* (Ridley, 2011). Morphological analyses of blood vessels in mouse and zebrafish models of angiogenesis have revealed that filopodia are the most prominent protrusions formed by endothelial tip cells (Gerhardt et al., 2003; Isogai et al., 2003). As shown in this study through time-lapse imaging, ECs also form blebs and lamellipodia. Membrane bleb formation was frequently detected prior to cytokinesis and may function to stabilise cell shape by acting as valves releasing cortical contractility to aid cytokinesis (Sedzinski et al., 2011). We also observed lamellipodia protrusions from filopodia during cell migration, highlighting the plasticity of ECs in generating different membrane protrusions to enable blood vessel growth. Furthermore, when depleted of filopodia by low Lat. B treatment, endothelial tip cells produce lamellipodia at the leading edge that are sufficient to propel the cell and vascular sprout forward. However, lamellipodia are less efficient in generating movement, as ECs migrate at decreased velocity. These findings suggest that ECs require at least two protrusive structures – filopodia and lamellipodia – that work cooperatively at the leading edge, with the former serving as a precursor structure for the generation of multiple lamellipodia to facilitate efficient migration *in vivo*.

Endothelial tip cells have been compared to axonal growth cones. Both structures protrude filopodia and respond to axon guidance molecules such as Slits and Roundabouts, Netrins and Unc5 receptors, Semaphorins, Plexins and Neuropilins, and Ephrins and Eph receptors (Adams and Eichmann, 2010). It should be noted, however, that neuronal guidance has been studied for over 100 years and the underlying mechanisms have been resolved in great detail through the investigation of widely accepted and specific guidance assays (Kolodkin and Tessier-Lavigne, 2011). By contrast, endothelial guidance has only been introduced over the past 10 years and is still comparatively ill-defined. Curiously, many of the conserved 'guidance' pathways that operate in growth cones serve to modulate the activity of the Vegf signalling pathway in ECs. Recent studies suggest that this might function to fine-tune the tip cell response to Vegf, which is the primary angiogenic cue for tip cell migration (Adams and Eichmann, 2010; Zygmunt et al., 2011). Our current study proposes another difference between neuronal growth cones and tip cells: although filopodia are required for the guided migration of growth cones (Bentley and Toroian-Raymond, 1986; Chien et al., 1993; Zheng et al., 1996), filopodia of endothelial tip cells are dispensable for their migration trajectory. By selectively inhibiting filopodia formation during sprouting angiogenesis under endogenous as well as ectopic signalling, we observed that ECs are still able to respond to, and migrate towards, external guidance cues in a directed manner. Hence, filopodia are not essential for guidance during EC migration. Instead, we show that they function as facilitators for efficient migration and vessel anastomosis. Finally, our findings raise further questions as to where guidance cues are received and where signalling is integrated in ECs during vessel patterning.

Competing interests statement
The authors declare no competing financial interests.

Author contributions
L.-K.P. designed and performed experiments, analyzed data and wrote the paper. H.G. designed experiments, analyzed data and wrote the paper. F.S. provided scientific support and edited the paper.

Supplementary material
Supplementary material available online at
http://dev.biologists.org/lookup/suppl/doi:10.1242/dev.097352/-/DC1

References
Adams, R. H. and Eichmann, A. (2010). Axon guidance molecules in vascular patterning. *Cold Spring Harb. Perspect. Biol.* **2**, a001875.
Arjonen, A., Kaukonen, R. and Ivaska, J. (2011). Filopodia and adhesion in cancer cell motility. *Cell Adh. Migr.* **5**, 421-430.

Bayless, K. J. and Johnson, G. A. (2011). Role of the cytoskeleton in formation and maintenance of angiogenic sprouts. *J. Vasc. Res.* **48**, 369-385.

Bentley, D. and Toroian-Raymond, A. (1986). Dioriented pathfinding by pioneer neurone growth cones deprived of filopodia by cytochalasin treatment. *Nature* **323**, 712-715.

Biyasheva, A., Svitkina, T., Kunda, P., Baum, B. and Borisy, G. (2004). Cascade pathway of filopodia formation downstream of SCAR. *J. Cell Sci.* **117**, 837-848.

Blum, Y., Belting, H.-G., Ellertsdottir, E., Herwig, L., Lüders, F. and Affolter, M. (2008). Complex cell rearrangements during intersegmental vessel sprouting and vessel fusion in the zebrafish embryo. *Dev. Biol.* **316**, 312-322.

Chhabra, E. S. and Higgs, H. N. (2007). The many faces of actin: matching assembly factors with cellular structures. *Nat. Cell Biol.* **9**, 1110-1121.

Chien, C. B., Rosenthal, D. E., Harris, W. A. and Holt, C. E. (1993). Navigational errors made by growth cones without filopodia in the embryonic Xenopus brain. *Neuron* **11**, 237-251.

Childs, S., Chen, J.-N., Garrity, D. M. and Fishman, M. C. (2002). Patterning of angiogenesis in the zebrafish embryo. *Development* **129**, 973-982.

Covassin, L. D., Villefranc, J. A., Kacergis, M. C., Weinstein, B. M. and Lawson, N. D. (2006). Distinct genetic interactions between multiple Vegf receptors are required for development of different blood vessel types in zebrafish. *Proc. Natl. Acad. Sci. USA* **103**, 6554-6559.

De Smet, F., Segura, I., De Bock, K., Hohensinner, P. J. and Carmeliet, P. (2009). Mechanisms of vessel branching: filopodia on endothelial tip cells lead the way. *Arterioscler. Thromb. Vasc. Biol.* **29**, 639-649.

Faix, J. and Rottner, K. (2006). The making of filopodia. *Curr. Opin. Cell Biol.* **18**, 18-25.

Fraccaroli, A., Franco, C. A., Rognoni, E., Neto, F., Rehberg, M., Aszodi, A., Wedlich-Söldner, R., Pohl, U., Gerhardt, H. and Montanez, E. (2012). Visualization of endothelial actin cytoskeleton in the mouse retina. *PLoS ONE* **7**, e47488.

Gerhardt, H., Golding, M., Fruttiger, M., Ruhrberg, C., Lundkvist, A., Abramsson, A., Jeltsch, M., Mitchell, C., Alitalo, K., Shima, D. et al. (2003). VEGF guides angiogenic sprouting utilizing endothelial tip cell filopodia. *J. Cell Biol.* **161**, 1163-1177.

Helbling, P. M., Saulnier, D. M. and Brändli, A. W. (2000). The receptor tyrosine kinase EphB4 and ephrin-B ligands restrict angiogenic growth of embryonic veins in Xenopus laevis. *Development* **127**, 269-278.

Herwig, L., Blum, Y., Krudewig, A., Ellertsdottir, E., Lenard, A., Belting, H.-G. and Affolter, M. (2011). Distinct cellular mechanisms of blood vessel fusion in the zebrafish embryo. *Curr. Biol.* **21**, 1942-1948.

Hogan, B. M., Bos, F. L., Bussmann, J., Witte, M., Chi, N. C., Duckers, H. J. and Schulte-Merker, S. (2009a). Ccbe1 is required for embryonic lymphangiogenesis and venous sprouting. *Nat. Genet.* **41**, 396-398.

Hogan, B. M., Herpers, R., Witte, M., Heloterä, H., Alitalo, K., Duckers, H. J. and Schulte-Merker, S. (2009b). Vegfc/Flt4 signalling is suppressed by Dll4 in developing zebrafish intersegmental arteries. *Development* **136**, 4001-4009.

Isogai, S., Horiguchi, M. and Weinstein, B. M. (2001). The vascular anatomy of the developing zebrafish: an atlas of embryonic and early larval development. *Dev. Biol.* **230**, 278-301.

Isogai, S., Lawson, N. D., Torrealday, S., Horiguchi, M. and Weinstein, B. M. (2003). Angiogenic network formation in the developing vertebrate trunk. *Development* **130**, 5281-5290.

Jacinto, A., Wood, W., Balayo, T., Turmaine, M., Martinez-Arias, A. and Martin, P. (2000). Dynamic actin-based epithelial adhesion and cell matching during Drosophila dorsal closure. *Curr. Biol.* **10**, 1420-1426.

Kapustina, M., Elston, T. C. and Jacobson, K. (2013). Compression and dilation of the membrane-cortex layer generates rapid changes in cell shape. *J. Cell Biol.* **200**, 95-108.

Kim, J.-D., Kang, H., Larrivée, B., Lee, M. Y., Mettlen, M., Schmid, S. L., Roman, B. L., Qyang, Y., Eichmann, A. and Jin, S.-W. (2012). Context-dependent proangiogenic function of bone morphogenetic protein signaling is mediated by disabled homolog 2. *Dev. Cell* **23**, 441-448.

Kimmel, C. B., Ballard, W. W., Kimmel, S. R., Ullmann, B. and Schilling, T. F. (1995). Stages of embryonic development of the zebrafish. *Dev. Dyn.* **203**, 253-310.

Kolodkin, A. L. and Tessier-Lavigne, M. (2011). Mechanisms and molecules of neuronal wiring: a primer. *Cold Spring Harb. Perspect. Biol.* **3**, a001727.

Krueger, J., Liu, D., Scholz, K., Zimmer, A., Shi, Y., Klein, C., Siekmann, A., Schulte-Merker, S., Cudmore, M., Ahmed, A. et al. (2011). Flt1 acts as a negative regulator of tip cell formation and branching morphogenesis in the zebrafish embryo. *Development* **138**, 2111-2120.

Kwan, K. M., Fujimoto, E., Grabher, C., Mangum, B. D., Hardy, M. E., Campbell, D. S., Parant, J. M., Yost, H. J., Kanki, J. P. and Chien, C.-B. (2007). The Tol2kit: a multisite gateway-based construction kit for Tol2 transposon transgenesis constructs. *Dev. Dyn.* **236**, 3088-3099.

Lawson, N. D. and Weinstein, B. M. (2002). In vivo imaging of embryonic vascular development using transgenic zebrafish. *Dev. Biol.* **248**, 307-318.

Leslie, J. D., Ariza-McNaughton, L., Bermange, A. L., McAdow, R., Johnson, S. L. and Lewis, J. (2007). Endothelial signalling by the Notch ligand Delta-like 4 restricts angiogenesis. *Development* **134**, 839-844.

Lu, X., Le Noble, F., Yuan, L., Jiang, Q., De Lafarge, B., Sugiyama, D., Bréant, C., Claes, F., De Smet, F., Thomas, J.-L. et al. (2004). The netrin receptor UNC5B mediates guidance events controlling morphogenesis of the vascular system. *Nature* **432**, 179-186.

Mattila, P. K. and Lappalainen, P. (2008). Filopodia: molecular architecture and cellular functions. *Nat. Rev. Mol. Cell Biol.* **9**, 446-454.

Mellor, H. (2010). The role of formins in filopodia formation. *Biochim. Biophys. Acta* **1803**, 191-200.

Millard, T. H. and Martin, P. (2008). Dynamic analysis of filopodial interactions during the zippering phase of Drosophila dorsal closure. *Development* **135**, 621-626.

Morton, W. M., Ayscough, K. R. and McLaughlin, P. J. (2000). Latrunculin alters the actin-monomer subunit interface to prevent polymerization. *Nat. Cell Biol.* **2**, 376-378.

Phng, L. K. and Gerhardt, H. (2009). Angiogenesis: a team effort coordinated by notch. *Dev. Cell* **16**, 196-208.

Pollard, T. D. and Cooper, J. A. (2009). Actin, a central player in cell shape and movement. *Science* **326**, 1208-1212.

Preibisch, S., Saalfeld, S. and Tomancak, P. (2009). Globally optimal stitching of tiled 3D microscopic image acquisitions. *Bioinformatics* **25**, 1463-1465.

Ridley, A. J. (2011). Life at the leading edge. *Cell* **145**, 1012-1022.

Riedl, J., Crevenna, A. H., Kessenbrock, K., Yu, J. H., Neukirchen, D., Bista, M., Bradke, F., Jenne, D., Holak, T. A., Werb, Z. et al. (2008). Lifeact: a versatile marker to visualize F-actin. *Nat. Methods* **5**, 605-607.

Riedl, J., Flynn, K. C., Raducanu, A., Gärtner, F., Beck, G., Bösl, M., Bradke, F., Massberg, S., Aszodi, A., Sixt, M. et al. (2010). Lifeact mice for studying F-actin dynamics. *Nat. Methods* **7**, 168-169.

Roman, B. L., Pham, V. N., Lawson, N. D., Kulik, M., Childs, S., Lekven, A. C., Garrity, D. M., Moon, R. T., Fishman, M. C., Lechleider, R. J. et al. (2002). Disruption of acvrl1 increases endothelial cell number in zebrafish cranial vessels. *Development* **129**, 3009-3019.

Rymo, S. F., Gerhardt, H., Wolfhagen Sand, F., Lang, R., Uv, A. and Betsholtz, C. (2011). A two-way communication between microglial cells and angiogenic sprouts regulates angiogenesis in aortic ring cultures. *PLoS ONE* **6**, e15846.

Salbreux, G., Charras, G. and Paluch, E. (2012). Actin cortex mechanics and cellular morphogenesis. *Trends Cell Biol.* **22**, 536-545.

Schäfer, C., Faust, U., Kirchgeßner, N., Merkel, R. and Hoffmann, B. (2011). The filopodium: a stable structure with highly regulated repetitive cycles of elongation and persistence depending on the actin cross-linker fascin. *Cell Adh. Migr.* **5**, 431-438.

Sedzinski, J., Biro, M., Oswald, A., Tinevez, J.-Y., Salbreux, G. and Paluch, E. (2011). Polar actomyosin contractility destabilizes the position of the cytokinetic furrow. *Nature* **476**, 462-466.

Siekmann, A. F. and Lawson, N. D. (2007). Notch signalling limits angiogenic cell behaviour in developing zebrafish arteries. *Nature* **445**, 781-784.

Thévenaz, P., Ruttimann, U. E. and Unser, M. (1998). A pyramid approach to subpixel registration based on intensity. *IEEE Trans.* **7**, 27-41.

Torres-Vázquez, J., Gitler, A. D., Fraser, S. D., Berk, J. D., Pham, Van N., Fishman, M. C., Childs, S., Epstein, J. A., Weinstein, B. M. (2004). Semaphorin-plexin signaling guides patterning of the developing vasculature. *Dev. Cell* **7**, 117-123.

Wiley, D. M., Kim, J.-D., Hao, J., Hong, C. C., Bautch, V. L. and Jin, S.-W. (2011). Distinct signalling pathways regulate sprouting angiogenesis from the dorsal aorta and the axial vein. *Nat. Cell Biol.* **13**, 686-692.

Wright, L. P. and Philips, M. R. (2006). Thematic review series: lipid posttranslational modifications. CAAX modification and membrane targeting of Ras. *J. Lipid Res.* **47**, 883-891.

Yoo, S. K., Deng, Q., Cavnar, P. J., Wu, Y. I., Hahn, K. M. and Huttenlocher, A. (2010). Differential regulation of protrusion and polarity by PI3K during neutrophil motility in live zebrafish. *Dev. Cell* **18**, 226-236.

Zheng, J. Q., Wan, J. J. and Poo, M. M. (1996). Essential role of filopodia in chemotropic turning of nerve growth cone induced by a glutamate gradient. *J. Neurosci.* **16**, 1140-1149.

Zygmunt, T., Gay, C. M., Blondelle, J., Singh, M. K., Flaherty, K. M., Means, P. C., Herwig, L., Krudewig, A., Belting, H.-G., Affolter, M. et al. (2011). Semaphorin-PlexinD1 signaling limits angiogenic potential via the VEGF decoy receptor sFlt1. *Dev. Cell* **21**, 301-314.